Journal of Physics: Conference Series

PAPER • OPEN ACCESS

Effect of Back Boundary Condition on Pyrolysis of Charring and Non-charring Materials

To cite this article: S Sabarilal and Amit Kumar 2018 *J. Phys.: Conf. Ser.* **1107** 032024

3rd European Symposium on Fire Safety Science IOP Publishing
IOP Conf. Series: Journal of Physics: Conf. Series **1107** (2018) 032024 doi:10.1088/1742-6596/1107/3/032024

Effect of Back Boundary Condition on Pyrolysis of Charring and Non-charring Materials

Sabarilal S[1], Amit Kumar[2]

National Centre for Combustion Research & Development & Department of Aerospace Engineering,
Indian Institute of Technology Madras,
Chennai, Tamil Nadu, India

sabarilals@gmail.com

ABSTRACT

Predicting pyrolysate fuel generation rate form a condensed fuel is an important component of fire models. For validating or tuning these subgrid models, mass loss rate (MLR) of small samples exposed to known radiant heat flux is measured in standard devices such as the cone calorimeter and Fire Propagation Apparatus (FPA). In order to accurately predict the MLR, pyrolysis model input parameters should represent actual fuel degradation process. The pyrolysis process is intricately coupled to heat transfer in the fuel. A few experimental studies on non-charring polymers [1][2] have shown that these results are sensitive to back boundary, therefore, special care should be taken in interpreting results from these bench-scale instruments. To elucidate the effect of back boundary on the pyrolysis process, here a numerical investigation is carried out for both charring and non-charring fuel material. In this work heat transfer process into the fuel is determined to understand the pyrolysis process. Heat transfer process in the two categories of fuel are quite different. For each fuel category study is carried out for 1 mm and 10 mm thick fuels exposed to low (20kW) and high (100 kW) fluxes. This work aims improve the understanding of burning process in these bench-scale instruments especially for charring substances which have not been addressed in literature in this regard. The study shed important insight for proper use bench tests as a versatile tool for fire safety engineers.

Keywords: *Cone calorimeter, FPA, back boundary, fire behaviour, pyrolysis, charring material, non-charring material, thin and thick fuel, burning process.*

NOMENCLATURE LISTING

A	Pre-exponential factor (1/s)	**Greek**	
Cp	Specific heat (J/kg/K)	κ	Absorption coefficient (m^{-1})
dz	Cell thickness (mm)	η	Surface transmissivity
E_a	Activation energy (J/mol)	σ	Stefan-Boltzmann constant ($W/m^2/K^4$)
h	Convective heat transfer coefficient ($W/m^2/K$)	ρ	Density (kg/m^3)
H_p	Heat of pyrolysis (s^{-1})	ε	Emissivity
k	Thermal conductivity (W/m/K)	**Subscripts**	
n	Order of reaction	v	Virgin fuel
T	Temperature (K)	c	Char
		i	ith computational cell

INTRODUCTION

In the recent years a number of pyrolysis models are developed to predict the production rate of gaseous fuel from condense phase fuel subjected to external heat flux[3][4].Pyrolysis modeling is complex since many of the input parameters are not known with high accuracy. Also current flammability test fails to provide all input parameter required for modelling[4]. An important drawback of current bench scale (FPA and cone calorimeter) test methods is that it fails to exactly define the thermal boundary condition at the rear face of the sample. To understand the pyrolysis process in detail the heat transfer across the entire fuel is essential. As per standard test the rear surface of the sample is insulated. To understand the heat transfer phenomena in standard configuration we need to consider entire assembly of sample and insulation also need to account for thermal contact resistance at interface along with this variation of insulation properties which make this job extremely complex and uncertain.[1] Suggests a well-defined back boundary condition by placing highly conductive inert material (aluminum block) and by introducing thermocouple into the block heat transfer across the back boundary during the test can be estimated. In this study same approach is adopted by introducing aluminum block at the back side of specimen and the variation in material behavior against standard configuration (insulated boundary condition) is investigated numerically. This work fuel of two thicknesses 1 mm and 10 mm is studied for both charring and non-charring fuels. The fuel is considered exposed to two heat fluxes, high (100 kW) and low (20 kW).

NUMERICAL MODELING

A simplified 1D pyrolysis model was developed based on principle of conservation of mass and energy similar to the way described in [4] is used to predict the pyrolysis of charring and non-charring material**.** A control volume approach is employed and the governing mass and energy conservation equations are solved numerically using a fully implicit scheme. In this present study 3 species (virgin solid, char, and pyrolysate) are considered and for charring and 2 species (virgin solid and pyrolysate) for non-charring material. The decomposition of virgin solid to pyrolysate takes place through a single step nth order Arrhenius type endothermic reaction. Pyrolysis gas is assumed to be in thermal equilibrium with the solid and escape immediately once it is formed so that no pressure buildup within the solid.

Thermal Balance and Governing Equations

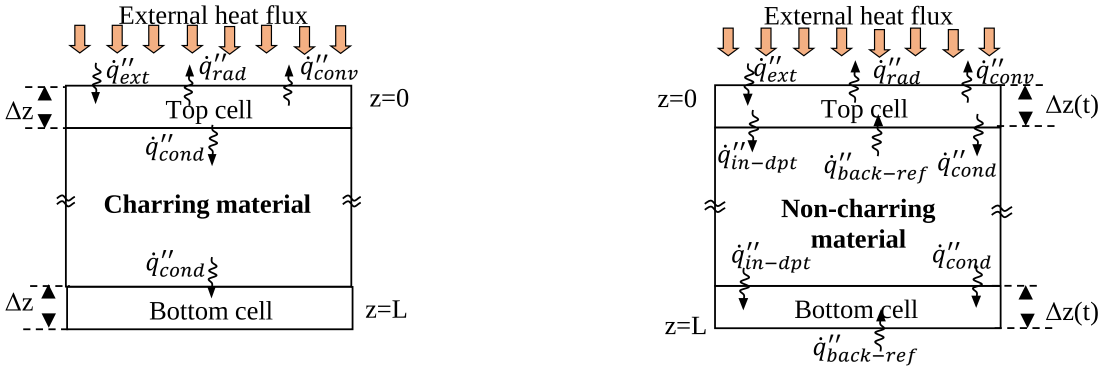

Fig. 1 Schematic of thermal boundary condition for charring and non-charring material.

$$\frac{\partial(\rho C_p T)}{\partial t} = \frac{\partial}{\partial z}\left(k\frac{\partial T}{\partial z}\right) - \dot{m}''' H_p \tag{1}$$

$$\frac{\partial(\rho C_p T)}{\partial t} = \frac{\partial}{\partial z}\left(k\frac{\partial T}{\partial z}\right) + \frac{\partial \dot{q}''_r}{\partial z} - \dot{m}''' H_p \tag{2}$$

Fig 1 shows schematic of energy balance for charring and non-charring material. In case of charring material the surface is assumed to be completely opaque so that external heat flux ($\dot{q}''_{ext}$) is first absorbed at the surface and energy is then conducted (q_{cond}) into the fuel. The radiation absorbed will be $\varepsilon\dot{q}''_{ext}$ since emissivity and absorptivity are considered same. Were ε is effective emissivity, which is evaluated using volume fractions of virgin material and char present at the surface. Similarly approach is adopted for evaluating effective thermal conductivity (k) and density (ρ) but effective specific heat (C_p) is evaluated using mass fractions. $\dot{q}''_{rad}$ and $\dot{q}''_{conv}$ represent the radiation and convection losses from surface.

Special consideration is taken for boundary condition of the non-charring semi-transparent material. For these kinds of materials a fraction of the applied external radiation ($\dot{q}''_{ext}$) is absorbed in-depth ($\dot{q}''_{in-dpt}$) according to its surface transmissivity and absorption coefficient. Unlike in charring material the energy is transported in semi-transparent material by in-depth absorption and conduction. As compared to other pyrolysis models for non-charring material this work considers in-depth emission along with in-depth absorption by solving RTE equation this additional term is given as $\frac{\partial \dot{q}''_r}{\partial z}$ in equation(2). The transmitted radiation which reaches the back boundary is reflected back ($\dot{q}''_{back-ref}$) based on the reflectivity of back surface. Further this reflected radiation is again absorbed and finally leaves the top surface of specimen. After considering in-depth emission and absorption, radiation leaving the cell $E(i)$ can be evaluated using equation (3), $E(i-1)$ is radiation entering the cell.

$$E(i) = E(i-1)e^{-\kappa dz(i)} - \sigma T_i^4\left(1 - e^{-\kappa dz(i)}\right) \tag{3}$$

NUMERICAL MODEL VALIDATION

The pyrolysis model developed is first validated against bench-scale experiments (FPA) of [5]. All the experiments in [5] were performed in 100% Nitrogen environment so that the thermal decomposition of fuel takes place in the absence of flame. Charring and non-charring pyrolysis models are validated against experiments conducted on chlorinated polyvinyl chloride (CPVC) and poly methyl methacrylate, PMMA respectively as shown in Fig. 2. Model input parameters for CPVC and black PMMA values are presented in Table 1.

Table 1 Model input parameters

	CPVC	PMMA		CPVC	PMMA		CPVC	PMMA
k_v	0.184 [5]	0.188 [6]	ρ_c	589.7 [5]	-	E_a	$2.5*10^5$ [5]	$1.64*10^5$[6]
ρ_v	1908.7 [5]	1190 [6]	Cp_c	1021.6 [5]	-	A	$7.9*10^{20}$ [5]	$2.5*10^{11}$ [6]
Cp_v	1933.8 [5]	1465 [6]	ε_c	1 [5]	-	H_p	$7.8*10^5$ [5]	$6.37*10^5$
ε_v	0.63 [5]	-	η	-	0.93 [6]	n	1.93 [5]	1
k_c	0.038 [5]	-	κ	-	960.5 [6]	h	10 [6]	10 [6]

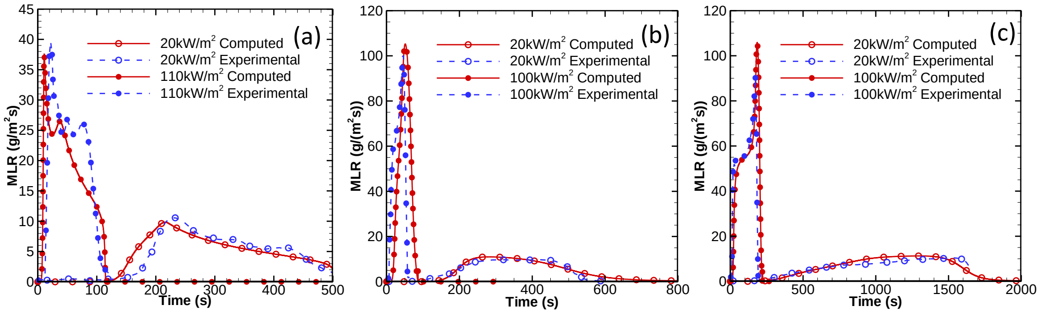

Fig. 2 Comparison between experimental [5] and numerical predictions. (a) 1.58 mm thick charring material (CPVC). (b) 3.18 mm thick non-charring material (PMMA). (c) 9.53 mm thick non-charring (PMMA) material.

MODIFIED BACK BOUNDARY CONDITION

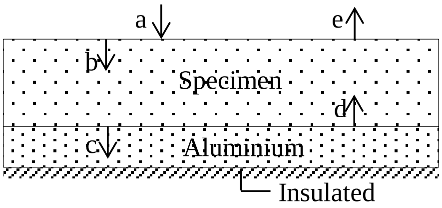

a	Incoming radiation
b	Radiation getting into specimen
c	Energy transferred to aluminium block
d	Back reflected radiation (only for translucent fuels)
e	Radiation leaving surface

Fig. 3 Schematic of modified boundary condition.

As mentioned before, one of the limitations of standard flammability test analysis (insulated boundary condition) is that it neglects the effect associated to back boundary of the sample. To understand the flammability nature of different material in more detail, understanding of energy transfer across the specimen especially the back surface is necessary. In this study a material of known thermal properties (Aluminum (Al) block) is introduced on the back side of the specimen as shown in Fig. 3 by doing this heat transfer to the block can be estimated and more robust and concrete pyrolysis model can be developed. For simulation aluminum block of 5mm thickness is considered with adiabatic back boundary and zero thermal contact resistance is assumed at the interface of specimen and Al block. For Al block thermal conductivity, specific heat and density are taken values 244 W/(mK), 921 J/(kg/K) and 2700 kg/m^3 respectively. Surface emissivity of 0.2 is taken for the block which is important in case of non-charring translucent fuel were in-depth radiation is considered.

RESULTS AND DISCUSSION

In this section the effect of back boundary on eight different cases are discussed, these include 1 mm and 10 mm thick fuel exposed to low (20 kW) and high (100 kW) heat flux each for charring and non-charring material. The cases of charring material are discussed first followed by cases for non-charring material.

Effect of back boundary on pyrolysis of charring material

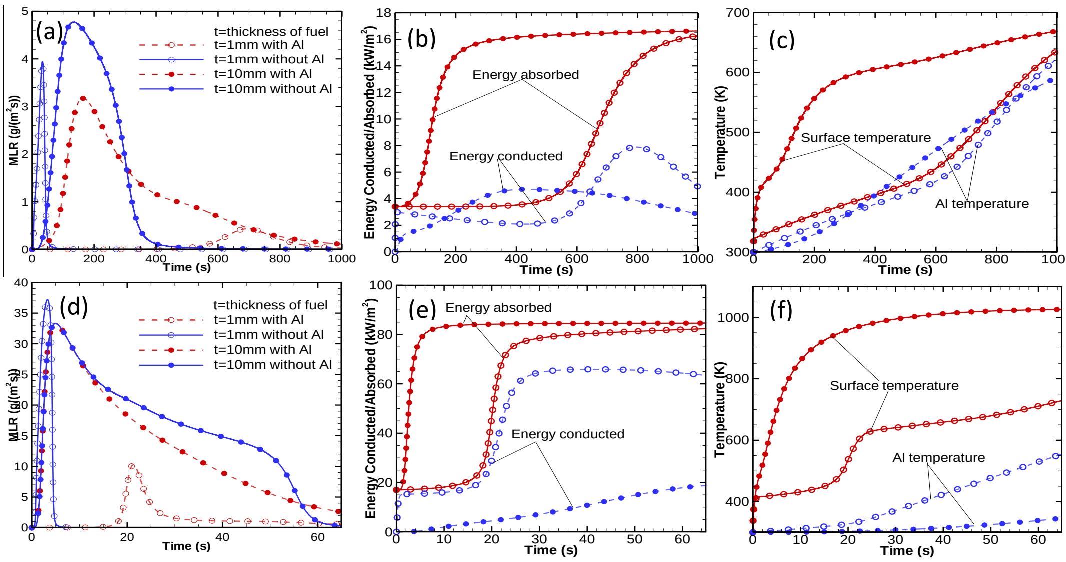

Fig. 4 Influence of thermal boundary condition on charring material pyrolysis (a),(b),(c) for 20 kW/m^2 and (d),(e),(f) for 100 kW/m^2. Clear circles represent thin fuel (1mm) and solid circles represent thick fuel (10mm). (a) and (d) MLR comparison with and without Al block. (b) and (e) Energy absorbed (solid line) and conducted (dashed line) to Al block during pyrolysis. (c) and (f) surface (solid line) and Al block (dashed line) temperature variation.

Fig. 4 shows influence of aluminum block on mass loss rate of charring material, as seen from Fig. 4(a) and (d) for 1 mm fuel, significant ignition delay was observed along with reduction in peak MLR. Because for 1 mm thick fuels the energy conducted to the aluminum block is high in the initial stages as seen in Fig. 4(b) and (e) and therefore, less energy will be available for sensible heating of the fuel and start the pyrolysis process. Once the specimen attains required temperature the pyrolysis process begins. During pyrolysis a char layer is formed on the specimen surface which increases the energy absorbed this is due to high surface absorptivity of char. As a result a sudden increase in absorbed energy and thereby an increase in energy conducted can be seen in Fig. 4 (b) and (e). For the four cases presented here, except for 100kw/m^2 on 10 mm thick fuel case all other show a delay in ignition. This is due to thermally thick and thermally thin nature of the fuel. In case of low heat flux (20kW/m^2) both 1mm and 10 mm act as thermally thin fuel. 1 mm fuel exposed to high heat flux (100kW) also behaves as thermally thin, since the thermal thickness is greater than material thickness prior to ignition.For the three thermally thin cases mentioned above from Fig. 4 (c) and (f) it is evident that the aluminum block temperature increases prior to MLR begins, this is due to the fact that the thermal wave travels faster than the pyrolysis. In case of 10 mm fuel exposed to high heat flux the heating rate is very high and due to higher material thickness the thermal wave takes more time to reach the back boundary that is why in Fig. 4 (f) the aluminum block temperature will not show an initial increase. As a result 10 mm fuel exposed to high heat flux act as thermally thick and will not show an ignition delay.

Effect of back boundary on pyrolysis of non-charring material

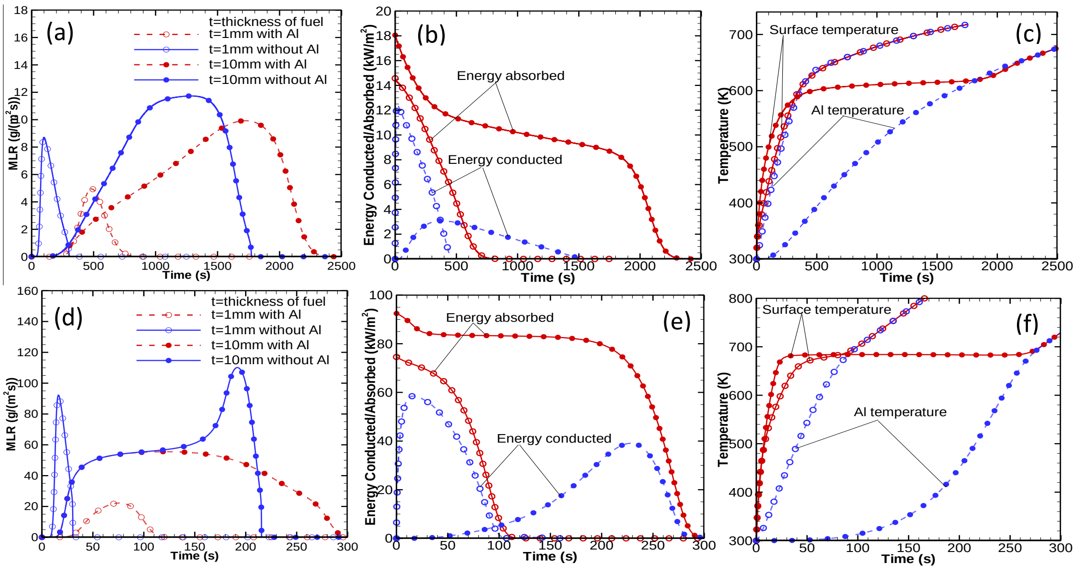

Fig. 5 Influence of thermal boundary condition on non-charring material pyrolysis (a),(b),(c) for 20kW/m^2 and (d),(e),(f) for 100kW/m^2. Open circles represent thin fuel (1mm) and solid circles represent thick fuel (10mm). (a) and (d) MLR comparison with and without Al block. (b) and (e) Energy absorbed (solid line) and conducted (dashed line) to Al block during pyrolysis. (c) and (f) surface (solid line) and Al block (dashed line) temperature variation.

Fig. 5 shows influence of aluminum block on mass loss rate of non-charring material, similar to charring material in Fig.4. One can note that pyrolysis in 1 mm thick fuel is more sensitive to back boundary conditions. One can see from Fig. 5 (a) for 1 mm fuel exposed to low heat flux (20 kW) significant ignition delay is observed. In charring material the only mode of heat transfer is by conduction as compared to non-charring translucent material where in-depth radiation also plays a role. This probably is the reason for higher sensitivity of 1 mm thick charring material to back boundary condition compared to 1 mm thick non-charring fuel. For all four cases the energy conducted to the aluminum block shows the same trend (initially increases and then decreases) during initial period the specimen temperature will be higher so heat conduction to aluminum increases, once the pyrolysis starts specimen thickness decreases and more radiation reaches aluminum block and its temperature increases results in a decrease in heat conduction as seen in Fig. 5 (b) and (e). As time progresses the specimen thickness decreases and energy absorbed also decreases but in case of charring material energy absorbed increases with time. In this case, the aluminum block temperature rise is due to two reasons heat conduction from specimen along with in-depth radiation which absorbed by aluminum surface, so toward the end of pyrolysis process (when specimen thickness is very less), the block temperature can be greater than specimen temperature as seen in Fig. 5 (c). Here also 1 mm and 10 mm thick fuel samples exposed to low heat flux and 1 mm thick fuel exposed to high heat flux behaves as thermally thin fuel and 10 mm thick fuel sample exposed to high heat flux behaves as thermally thick which is clear from Fig. 5 (e) and (f). Another interesting result observed in thick fuel exposed to high heat flux Fig. 5 (d) is that due to the introduction of aluminum block the peak in MLR disappears which was observed in insulated boundary condition. Similar experimental observation is reported for PA6 and HIPS[1][2] . When using insulated boundary condition this peak in MLR at the end of burning is caused due to the reduction in conduction heat flux to the specimen when the pyrolysis zone approaches the insulation back boundary. By introducing aluminum at the back boundary heat is transferred to the block even if the pyrolysis front reaches back boundary and peak disappears.

CONCLUSION

A 1D pyrolysis model validated against bench-scale tests is used to analyze the effect of back boundary on pyrolysis process of charring and non-charring material. By introducing an aluminum block, a delay in pyrolysis process is observed especially for thin fuels (here 1mm thick). In case of charring material and non-charring material 1 mm and 10 mm thick fuel samples exposed to low heat flux (20 kW/m^2) and 1 mm thick fuel exposed to high heat flux (100 kW/m^2) behaves as thermally thin and 10 mm thick fuel sample exposed to high heat flux (100 kW/m^2) behaves as thermally thick fuel. When 10 mm thick non-charring material exposed to higher heat flux a sudden peak in MLR is observed towards the end of pyrolysis is not a material property, it is an after effect of insulated back boundary condition. The main intention of introducing the aluminum block at the back side of the sample is to quantify the heat transfer across the rear side and those experimental data can be better fitted with numerical models thereby a better understanding of pyrolysis process.

REFERENCES

[1] R. Carvel, T. Steinhaus, G. Rein, and J. L. Torero, “Determination of the flammability properties of polymeric materials: A novel method,” *Polym. Degrad. Stab.*, vol. 96, no. 3, pp. 314–319, 2011, 10.1016/j.polymdegradstab.2010.08.010

[2] B. Schartel, M. Bartholmai, and U. Knoll, “Some comments on the use of cone calorimeter data,” *Polymer Degradaton and Stability.*, vol. 88, no. 3, pp. 540–547, 2005, 10.1016/j.polymdegradstab.2004.12.016

[3] S. I. Stoliarov, S. Crowley, R. N. Walters, and R. E. Lyon, “Prediction of the burning rates of charring polymers,” *Combustion and Flame*, vol. 157, no. 11, pp. 2024–2034, 2010, 10.1016/j.combustflame.2010.03.011

[4] C. Lautenberger and C. Fernandez-pello, A Generalized Pyrolysis Model for Combustible Solids, no. April. *Fire Safety Journal*, 2007, 10.1016/j.firesaf.2009.03.011

[5] M. Chaos, M. M. Khan, N. Krishnamoorthy, J. L. De Ris, and S. B. Dorofeev, “Evaluation of optimization schemes and determination of solid fuel properties for CFD fire models using bench-scale pyrolysis tests,” *Proceedings of the Combustion Institute.*, vol. 33, no. 2, pp. 2599–2606, 2011, 10.1016/j.proci.2010.07.018

[6] N. Bal and G. Rein, “Numerical investigation of the ignition delay time of a translucent solid at high radiant heat fluxes,” *Combustion and Flame*, vol. 158, no. 6, pp. 1109–1116, 2011, 10.1016/j.combustflame.2010.10.014